DOI: 10.13009/EUCASS2023-377
Aerospace Europe Conference 2023 – 10TH EUCASS – 9TH CEAS

Investigating potentials of active flow control via retrofit of commercial aircraft

Valerio Mosca[⋆], *Stanislav Karpuk*[†] *and Ali Elham*[††]
[⋆†]*Institute of Aircraft Design and Lightweight Structures, Cluster of Excellence SE*^{2}*A*
Technische Universität Braunschweig, Braunschweig 38108, Germany
[††]*Department of Aeronautics and Astronautics, Computational Engineering and Design Group*
University of Southampton, Southampton SO16 7QF, United Kingdom
v.mosca@tu-braunschweig.de · s.karpuk@tu-braunschweig.de · A.Elham@soton.ac.uk
[⋆]Corresponding author

Abstract

Hybrid Laminar Flow Control (HLFC) remains one of the most promising airframe technologies that can substantially improve overall aircraft efficiency. Although many numerical and experimental studies investigated the capabilities of HLFC, it is still challenging to consider the technology in a conceptual aircraft design phase. The present work focuses on integrating novel methodology for HLFC in the conceptual design with overall aircraft design to investigate the potential of HLFC on performance improvement of commercial aircraft. In particular, three commercial aircraft are studied and optimized aerodynamically for turbulent and HLFC applications, correlations are derived.

1. Introduction

European governments are developing a strategy to significantly reduce emissions in various industries. Similar to many other industries, the aviation sector is focusing on various ways to minimize adverse environmental impacts. Solutions include improvements in airframe technologies to make them more efficient, the development of more energy-efficient propulsion systems, and explorations of new more environmentally-friendly energy sources. To motivate further developments in the direction of lower emissions, Flightpath 2050[1] set potential goals for the future of aviation, such as 75% and 90% reduction of CO_2 and NO_x emission, respectively, and a 65% noise reduction. To investigate potentially disruptive airframe, propulsion, and energy technologies, the Cluster of Excellence SE^{2}A (Sustainable and Energy Efficient Aviation)[2] was initiated in 2019. The SE^{2}A is an interdisciplinary research center developed in Germany to accomplish the above-mentioned objectives for sustainable aviation by investigating different technologies. The cluster combines various research groups from TU Braunschweig, DLR, and Leibniz University in Hannover to investigate, quantify, and give recommendations regarding future technologies, their applicability, and the challenges of their implementation. A possible solution to significantly reduce emissions for future aircraft would be to improve the overall airframe efficiency. Those solutions are mainly targeted to reduce aircraft drag. Depending on the drag component to be reduced, various solutions can be implemented. Reduction of parasite drag still remains a challenging task, although significant effort has been put in for decades. The most promising technology to drastically reduce parasite drag is to control the boundary layer. Particularly, an extension of the laminar boundary layer may substantially reduce the overall drag of the aircraft and change the overall aircraft performance and emissions via the snowball effect.[3] In fact, laminar flow control may be one of the most powerful airframe technologies to significantly reduce fuel burn and emissions to achieve given goals.[4] Two major options for laminar flow control of wing sections exist. Natural Laminar Flow (NLF) airfoils are characterized by a proper shape design to reach laminar flow passively. The second option utilizes the use of Boundary Layer Suction (BLS) to reduce drag and hence improve aerodynamic efficiency to minimize fuel weight. The technique removes a small amount of flow at low momentum in the near-wall region to mitigate adverse effects of Tollmien–Schlichting (TSI) and Cross Flow (CFI) instabilities. This technique gives more potential to laminarize the flow, especially for cases of high sweep angle and Reynolds number, where NLF solutions are no longer possible. The couple of BLS with NLF creates a so-called Hybrid Laminar Flow Control (HLFC). This way, the benefits of both systems can be utilized, and a rather limited portion of BLS is required. An overview of the HLFC application in different experimental tests is presented in Krishnan et al.[5] Moreover, several experimental campaigns have been performed to evaluate the potential benefits of HLFC for commercial aircraft. In Henke,[6] the flight test of the A320 vertical tail equipped with HLFC is presented. Different recent design and sensitivity

DOI: 10.13009/EUCASS2023-377

studies have been done using HLFC showing promising results. Beck et al.[3] investigated the potential of laminar flow control on a mid-range forward-swept wing, achieving fuel burn reduction of about 47% thanks to 80% of laminar flow on the wing while the fuselage showed a potential of 70% laminar flow. Sudhi et al. performed different series of 2D airfoil shape optimizations from subsonic[7] to transonic regimes.[8] In the transonic regime, NLF and HLFC configurations have been explored. The optimum NLF airfoil has 27% lower drag than an optimum turbulent airfoil, while the optimum HLFC airfoil showed a 25% lower total drag than the NLF airfoil.[8] A complete wing configuration performing aerostructural optimization and considering the rest of the aircraft is presented in Mosca et al.[9] A fully electric short-range airplane with HLFC has been optimized, showing a reduction of profile drag of more than 38%.

To address the potential benefits of HLFC for future aircraft, proper treatment of the technology from the fidelity standpoint needs to be done. Generally, different aerostructural analysis and optimization frameworks can be adopted in aircraft design, ranging from low- to high-fidelity. Low-fidelity tools present a reduced demand for computational power, making them suitable for preliminary aircraft design[4] but subject to some inaccuracies due to simplified models implemented. On the other hand, high-fidelity solutions can be applied to capture detailed phenomena in the aerodynamic and structural field, which is useful for design improvements and improving accuracy. Nevertheless, the application of those can be limited because of the lack of proper computational power and expertise in their application. In Kenway et al.,[10] multi-point high-fidelity aerostructural optimizations are performed. In fact, a full long-range aircraft is analyzed using Euler Computational Fluid Dynamics (CFD) and a structural finite element model with 300 000 degrees of freedom. The coupled adjoint sensitivity method was implemented for gradient computation. The analysis needed a parallel supercomputer to be able to perform such solutions. Hence, a medium-fidelity approach represents a trade-off between acceptable computational resources and accuracy in the analysis.

This work presents an investigation of the potential benefits of HLFC technology to current commercial aircraft using a multi-fidelity approach. Three standard aircraft with various payloads and ranges are digitized to be further used for the HLFC assessment: Fokker F70, Airbus A220, and Airbus A320. Once all the performance and weight parameters are obtained, a medium-fidelity framework for aerostructural optimization is used to optimize the airfoil shapes of the wing and HLFC suction properties. The aim is to provide valuable correlations to be applied in the early design phase considering the HLFC technology and respecting the practical design and operational constraints of current aircraft.

The present work is divided into several sections. Section II describes the methodology of reference aircraft initialization and sizing using the reverse engineering approach, while section III describes the multidisciplinary design optimization framework which implements the HLFC technology. Finally, Section IV discusses optimization results and the correlations found. In the last section, conclusions are determined.

2. Reference aircraft definition and preliminary analysis

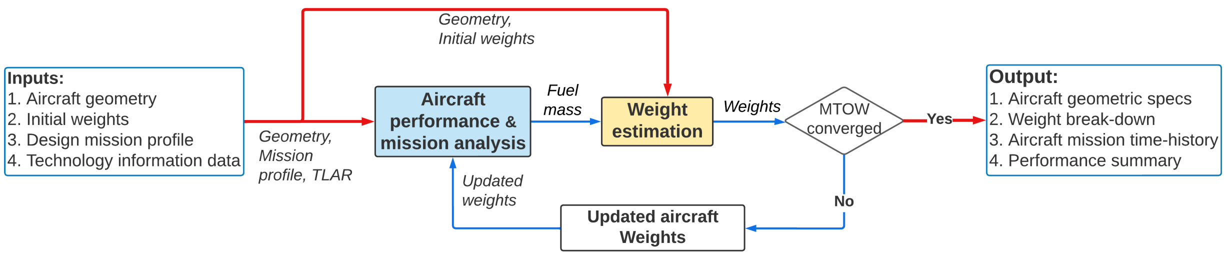

Figure 1: Initial sizing flowchart using SUAVE. Red lines indicate single data transfer while blue lines show the iterative loop data transfer.

The sizing process presented here helps obtain the mission performance data throughout the mission and the preliminary weights of components required for further HLFC assessments. To evaluate the potential benefits of HLFC technologies on given aircraft, their initial geometric properties, weights, and performance characteristics shall be obtained. Planforms of all airplanes were initially digitized using 3-view drawings to obtain basic geometric properties required for the aerodynamic analysis. Since no information regarding specific airfoils for each aircraft is available, typical airfoils for given flight conditions were used. In the present work, DLR F15 airfoil was used as a reference one and was scaled and twisted based on typical thickness distributions provided by Obert.[11] Generic characteristics of the propulsion system, such as geometry, pressure and bypass ratios, and others, were obtained from open sources. All obtained information was implemented in the initial sizing framework based on the mission analysis software

DOI: 10.13009/EUCASS2023-377

SUAVE.[12] The sizing framework flowchart is shown in Fig.1. There, the initially prescribed data is used for the performance and mission analysis module that includes take-off and landing physics-based analyses using the method of Gudmundsson[13] and a time-dependent mission simulation based on equations of motion. The aerodynamic analysis required for the mission analysis is performed using a combination of AVL vortex-lattice method[14] for lift and induced drag, and semi-empirical methods for parasite and compressibility drag and the Oswald efficiency.[13,15,16] The aircraft drag is defined by

$$C_D = C_{D_p} + C_{D_i} + C_{D_c} + C_{D_{misc}} \tag{1}$$

where C_{D_p} is the parasite drag estimated using the method of Gudmundsson,[13] C_{D_c} is the compressibility drag defined using the method of Shevell,[15] $C_{D_{misc}}$ is the miscellaneous drag, and C_{D_i} is the induced drag defined by

$$C_{D_i} = C_L^2 \left(\frac{1}{\pi k_{e,F} e_{theo} AR} + k_{visc} C_{D_p} \right) \tag{2}$$

where e_{theo} is the span efficiency obtained from AVL and k_{visc} is the correction factor responsible for viscous effects and $k_{e,F}$ is the fuselage correction factor.[16] C_L represents the lift coefficient, while AR is the aspect ratio.

After the mission and performance analyses are completed, and the required mission fuel weight is estimated, weight estimation is updated. The empty weight estimation is based on the component-breakdown method and uses two different methods. The wing weight is estimated using the physics-based EMWET method,[17] while other components are calculated using the semi-empirical FLOPS method.[18] After estimating the empty weight, the maximum takeoff weight (MTOW) is found by

$$MTOW = W_e + W_f + W_c + W_p \tag{3}$$

where W_e, W_f, and W_p are empty, fuel, and payload, respectively. After the weights are estimated, a deviation from the initial MTOW value is present. Therefore, all weights are updated and used again for the new mission analysis iteration. The process is repeated until the MTOM difference reaches the convergence criterion. Obtained results after the initial sizing are then checked with the actual data of reference aircraft. Particularly, weights and engine specific fuel consumption (SFC) are checked to ensure minimum deviations from the reference data. If proper digitalization of the geometry and extraction of the propulsion system and mission data is performed, few iterations are required for convergence, and minimum deviation is observed.

To obtain some parameters required for the mid-fidelity analysis, an initial aircraft sizing using HLFC assumptions need to be performed at the low-fidelity level as well. In this case, The transition Reynolds number for every section along the wing is estimated using the curve estimated by Hepperle[19] and shown in Fig. 7. The function that represents the theoretical boundary of the HLFC is defined by:

$$Re_T = \left(-4.444 \cdot 10^{-6} \varphi_{LE}^4 + 3.8545 \cdot 10^{-4} \varphi_{LE}^3 - 1.888 \cdot 10^{-2} \varphi_{LE}^2 + 3.5196 \cdot 10^{-2} \varphi_{LE} + 29.965\right) \cdot 10^6 \tag{4}$$

where φ_{LE} is the leading edge sweep angle. Given the chord Reynolds number for each section of interest, the transition location for both upper and lower surfaces are defined by:

$$X_{tr} = \min\left(\frac{Re_T}{Re}, 0.65\right) \tag{5}$$

where Re is the chord Reynolds number and the factor of 0.65 is defined as a practical limit of airfoil transition location to avoid the limitation of the formulation.

3. Multidisciplinary design optimization

After the initial analysis of reference aircraft is performed to evaluate their potential performance with and without the HLFC technology, the data moves to the Multidisciplinary Design Optimization (MDO) framework. The framework includes different modules: aerodynamic module, structural module, performance evaluation, and boundary layer suction system analysis. A genetic algorithm based available in Matlab is used for full aerostructural gradient-free optimization. Difficulties in the computation of variable derivatives and possible convergence issues make the choice for a gradient-based algorithm discouraging since the high robustness of the framework is required. The mutation scheme adopted is the ′mutation adapt feasible′. It randomly generates directions that are adaptive with respect to the last successful or unsuccessful generation. The mutation chooses a direction and a step length that satisfies bounds and constraints. A default crossover fraction of 0.8 is implemented. The optimization problem is written in the following

DOI: 10.13009/EUCASS2023-377

form:

$$\begin{aligned} \text{Minimize} \quad & W_f(X) \\ \text{w.r.t.} \quad & X = [cst_r\ cst_{b50\%}\ cst_k\ cst_t\ k_{suc_u}\ k_{suc_b}\ \epsilon_r\ \epsilon_k\ \epsilon_{b50\%}\ \epsilon_t] \\ \text{subject to} \quad & \left(V_f\right)_{req} \leq \left(V_f\right)_{av} \\ & X_{lower} \leq X \leq X_{upper} \end{aligned} \tag{6}$$

The fitness function is given by the fuel weight minimization W_f. The first four groups of design variables represent the evolved version of the Class Shape Transform (CST) method[20] that was proposed in origin by Kulfan.[21] In particular, they are implemented to define airfoil shape for the root, kink, 50% of the span, and tip sections. The variables k_{suc_u} and k_{suc_b} represent the suction scale coefficients for the upper and bottom surfaces, respectively. The parameters ϵ_r, ϵ_k, $\epsilon_{b50\%}$, and ϵ_t define the twist angles at the different sections. Each airfoil shape is defined through 10 design variables (5 for the upper surface and 5 for the lower one) and considering the other design variables, a total of 52 design variables characterize the optimization problem. The airfoils used as an initial reference to start the optimizations are obtained through a two-dimensional (2d) optimization, considering CSTs coordinates as design variables and the parameters defining the Bezier curve used for the suction distribution, minimizing the total drag, using a similar approach performed in Sudhi et al.[8] For example, in Fig.2, three airfoils are tested for a $C_l = 0.3$ and $Re = 15e6$, representing a potential section for the mid-span position of the wing. The third airfoil slightly reduces the laminar flow, but a weakening of the shock wave can be spotted in the pressure coefficient plot C_p, reducing the wave drag. In the top right plot of the figure, the suction distribution is shown. In particular, the local non-dimensionalized suction velocity v_0/U_∞ shows the suction profile for the upper and lower surface of the airfoils with respect to the non-dimensionalized coordinate x/c. The third airfoil presents higher suction drag, but this element is well compensated by the other reduced drag components, making it characterized by lower total drag (sum of friction, pressure, and suction drag). The initial

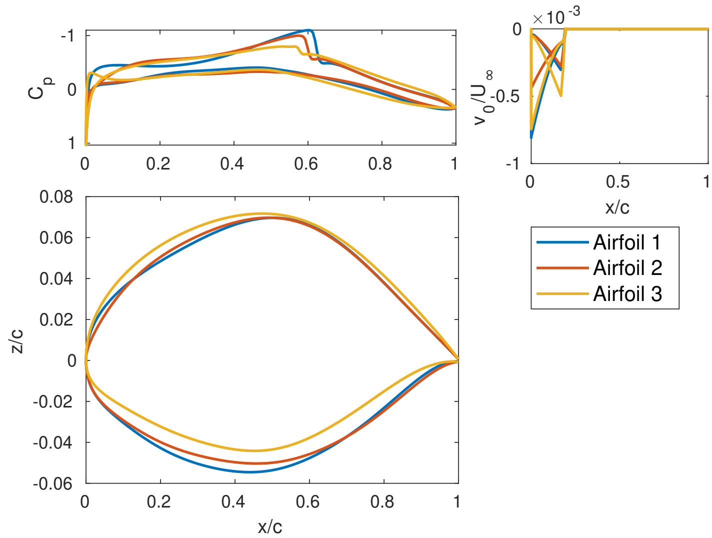

Figure 2: 2d airfoil optimization.

population is given by a data set of transonic and standard airfoils, while the other parameters are built using the Latin Hypercube sample matrix. The proposed wing optimization is performed at cruise conditions, but it is also important to consider the other flight segments and conditions. The only constraint used is given by the required fuel volume $\left(V_f\right)_{req}$ smaller or equal to the available one $\left(V_f\right)_{av}$.

The optimization framework is visualized through the eXtended Design Structure Matrix (XDSM)[22] in Fig.3, more details about the framework can be found in Mosca et al.[23] The Quasi-three-dimensional hybrid-laminar-flow-control (Q3D-HLFC) aerodynamic tool is used to calculate the distribution of lift and loads that are then used for EMWET[17] to obtain the wing weight for the maximum load factor of $n_{max} = 2.5$ based on certification requirements.[24] In this phase, the tool runs without computation of the drag (inviscid) to save computational time. Then, the Q3D-HLFC is run in a viscous mode, evaluating lift and drag coefficients for cruise condition ($n_{max} = 1$). The coefficients become the input of the performance module to determine fuel weight. The boundary layer suction routine receives suction drag and wing suction power parameters. It computes the total suction power of the wing and the rest of the

DOI: 10.13009/EUCASS2023-377

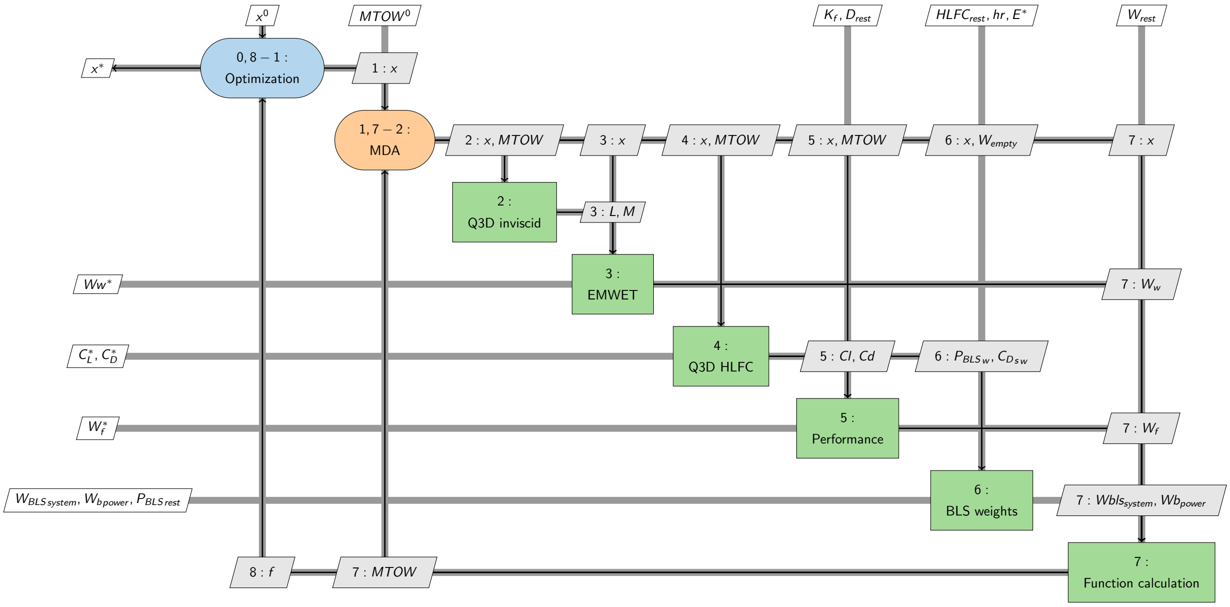

Figure 3: XDSM for wing optimization.[23]

aircraft to size a battery that will provide the demanded energy. Hence, the weight of the battery $W_{battery-power}$ and of the suction system $W_{suc-system}$ are computed. All the weights, including the weight of the rest of the aircraft besides the wing, not changing during optimization (W_{rest}), are summed together to obtain the maximum take-off weight (MTOW):

$$MTOW = W_w + W_f + W_{battery-power} + W_{suc-system} + W_{rest} \tag{7}$$

The iteration between the modules is stopped once the tolerance for each weight component is satisfied. To sum up, an initial aerodynamic airfoil shape optimization is performed for each aircraft to achieve proper airfoils optimized to minimize drag and suction power. In particular, different flight conditions are set, depending on the cruise altitude of the chosen case, together with lift coefficient and Reynolds number, depending on the position of the section along the span. Once optimized airfoils are obtained, they are used for full aerostructural optimization. The approximate computational time of such optimization is about 230 hr using a 48-core Intel Xeon(R) Gold 6252 CPU @ 2.10GHz.

3.1 Aerodynamic module

The aerodynamic module is characterized by the Quasi-Three-Dimensional Hybrid Laminar Flow Control (Q3D-HLFC) aerodynamic solver. The tool represents a modified version of the Quasi-Three-Dimensional (Q3D) tool.[25] The updated version presents the possibility of evaluating aerodynamic performance for NLF and HLFC cases. Besides, a so-called 2.75D approach is used.[26] According to this methodology, a conical transformation is used to define the two-dimensional sections. In order to move from two-dimensional to three-dimensional properties, the calculated shock-wave line is used as the reference sweep angle.[26,27] Drag components computed are friction, pressure (including wave drag), and induced drag. Because of the BLS system, another form of drag, called *suctiondrag* has to be considered. In fact, the technique implies an energetic dispense due to the pressure losses experienced in the system. The Q3D-HLFC is described in three steps. In the first step, a Vortex Lattice Method (VLM) is used to obtain the lift distribution along the wing span, aerodynamic load, and the lift coefficient C_L. Induced drag is also obtained. After that, the second step presents an aerodynamic airfoil analysis for each wing section. The wing is divided into different sections, each of which is analyzed by the coupling of MSES[28] and COCO-LILO.[29,30] MSES is a two-dimensional, steady, compressible Euler solver developed by Drela at MIT.[28] The tool is used to compute the friction drag component for the turbulent portion of the airfoil and for the pressure drag. Besides, the pressure distribution is obtained and fed to the COCO-LILO routine. The COnical, COmpressible (COCO) boundary layer solver was developed by Schrauf et al.[29] It receives the airfoil pressure distribution together with the suction distribution as input. The Newton method is applied to solve the boundary layer equation system. The solution yields the velocity and temperature profiles, together with their derivatives, necessary for the linear stability solver (LILO).[30] The boundary layer solver COCO also has the laminar skin friction drag as output. LILO applies linear stability theory to determine the amplification rates of the disturbance frequencies, as the solution of the eigenvalue problem of the Orr-Sommerfield equation.[30] The two N-factor

DOI: 10.13009/EUCASS2023-377

method is used to take into account the effect of Tollmien–Schlichting and Cross-flow instabilities in the transition to turbulent flow (a similar approach is used in[27]). The attachment-line-momentum-thickness Reynolds number $Re_{\theta,AL}$ is used to evaluate the attachment-line transition, using the methodology implemented by Pfenniger.[31,32] The 2d analysis is corrected through conical flow assumptions and a 2.75D methodology to consider the three-dimensional effect. The last step is characterized by the total drag computation, considering the induced drag from the first step and integrating the drag components for each section from the second step along the span. The same integration approach is used to compute the total suction power. More details about the Q3D-HLFC are present in Mosca et al.[23]

3.2 Structural module

The module computes the wing weight through the use of EMWET tool.[17] The methodology is characterized by wing decomposition in primary and secondary structures. In particular, inside the primary weight, the optimum and non-optimum structure weight is included. The optimum weight represents the weight of the wing box and its sizing through the amount of material necessary to sustain the critical loads. The non-optimum structure includes joints and attachments that, together with the secondary weight (given by components like leading and trailing edges, high lift devices, and movable), are obtained using empirical methods. EMWET is developed for conventional-metal wings, hence to take into account the effects of structure layout and novel materials necessary for boundary layer suction system, a reduction of 20% is applied. The use of composite materials is motivated by the requirement of having a high-quality surface with low waviness to enable optimal boundary layer performance after the suction region. The wing weight is computed by receiving as input the aerodynamic loads calculated by the Q3D-HLFC during step 1 (see Sec.3.1). The loads are obtained for a maximum load factor of 2.5. The tool presents good accuracy, estimating an error of 2%.[17] More details about EMWET are explained by Elham et al.[17]

3.3 BLS system module

The module evaluates the mass of the battery necessary to give enough power for the boundary layer suction. Besides, an estimation of the suction system components' weight is provided. The methodology used is presented in a detailed way in the work of Mosca et al.[23] The battery weight is given by:

$$W_{b_{power}} = \frac{(P_w + P_{rest}) \cdot hr}{E^*} \tag{8}$$

in which P_w represents the power necessary to apply suction on the wing, while P_{rest} gives the estimation of suction power for the rest of the aircraft (in this research, suction is limited to the main wing). The value hr is the number of hours for BLS application. It is estimated considering the cruise Mach number and the range of the applied case. The specific energy density E^* chosen is 700 Wh/kg as described in the work of Karpuk et al.[33] The weight of the suction system is computed for the wing only. The wing suction system weight is computed proportionally, using a methodology adopted by Karpuk et al.[4] where the vertical tail suction system is computed as a fraction of Operating Empty Weight (OWE) and values are obtained from several references.[34,35] The wing suction system weight is obtained taking into account the portion characterized by suction, spanwise and chordwise. In particular, the suction is limited by structural constraints given by the front spar, hence generally is designed for a 15-20% of the chord while along 75% of the span for the lifting surfaces. More details are provided by the work of Mosca et al.[23]

3.4 Performance module

The fuel weight W_f is computed inside this module. It takes into account the range of the designed mission that also includes the reserve (a 5% of the fuel weight is considered as reserve fuel). According to Roskam:[36]

$$W_f = 1.05(1 - M_{ff})MTOW \tag{9}$$

where M_{ff} is the total fuel weight fraction and $MTOW$ as the maximum take-off weight. It gives the estimation of the burnt fuel through the ratio between the total aircraft weight at the end of the mission to the initial one defined by:

$$M_{ff} = 0.9386 \cdot e^{\left(\frac{-K_{ff}}{L/D}\right)} \tag{10}$$

The fraction M_{ff} is determined from the Brequet equation for cruise mission, corrected with a coefficient 0.9386 for the other flight segments. The coefficient K_{ff} is related to the engine characteristics. It can be empirically found reversing Eq. (9) and Eq. (10) using data from the reference aircraft. The aerodynamic efficiency L/D is obtained considering the wing drag from the aerodynamic module and the drag of the aircraft besides the wing, fixed before optimization.

DOI: 10.13009/EUCASS2023-377

4. Results

Three different aircraft are considered for this research: Fokker F70, Airbus A220, and Airbus A320. They are digitized using the methodology presented in Sec.2 using low-fidelity methods. The first step in the digitalization process is to perform initial sizing and mission analysis of the aircraft in full turbulent mode to determine standard characteristics of the aircraft and ensure comparable results with the actual case, although not all data is available from operating manuals and brochures. Then, the HLFC system is taken into account for retrofitting the aircraft, since low-fidelity methods use AVL and EMWET as main tools, where the airfoil shape is considered and other analysis modules require only generic data. This way, it is assumed that the HLFC is implemented on the given wing, and an empirical correlation of Hepperle shown in Eq. (4) is used. Considering the presence of the suction system and its aerodynamic effects, a variation in performance and weight is expected. Therefore, the aircraft is resized accordingly using similar procedures. After the low-fidelity analysis, a medium-fidelity approach as described in Sec.3 is used. In particular, the implementation of the suction system requires at least a variation of the airfoil shape. This represents the minimum modification necessary to apply on the wing in order to have HLFC and satisfy most design constraints. Figure 4 presents the flowchart showing the steps performed.

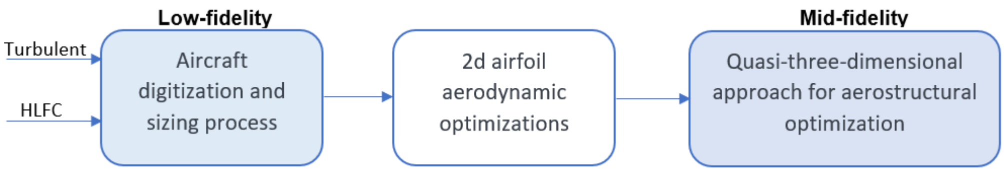

Figure 4: Optimization flowchart.

Tab.1 shows the results of the optimization for the Fokker F70. The aircraft equipped with optimized airfoils with boundary layer suction present a reduction of about 16% of the fuel weight W_f with respect to the configuration presenting optimized turbulent airfoil. The reduction is favored by an augmentation of the aerodynamic efficiency C_L/C_D. In fact, the wing drag coefficient ($C_{D_{wing}}$) is reduced by about 15.9% and compensating for the lower $C_{L_{cruise}}$, given by a reduction of the maximum take-off weight W_{TO}. $W_{b_{power}}$ represents the weight of the battery necessary to give the power needed for suction, while $W_{BLS_{tot}}$ is the weight of the suction system. These two components of weight are present in the configuration with BLS only.

Table 1: Optimization results for the F70.

	Turbulent opt.	**HLFC opt.**
$C_{L_{cruise}}$	0.3292	0.3115
C_L/C_D	15.5	17.4
$C_{D_{wing}}$	0.0111	0.0094
$\Delta C_{D_{wing}}$		-15.9%
W_w	4268 kg	3017 kg
$W_{b_{power}}$	0 kg	184 kg
$W_{BLS_{tot}}$	0 kg	203 kg
W_{TO}	42222 kg	39376 kg
W_f	9456 kg	7932 kg
ΔW_f		-16.1%

In Tab.2 and Tab.3 the optimization results comparing the two configuration suction-turbulent airfoils are shown for the Airbus A220 and A320. A similar reduction of the fuel weight and drag is achieved, proving that by keeping the same wing planform geometry and typical constraints of commercial aircraft, fuel weight, and wing drag can be reduced up to 16%. It must be noted that the present research assumes that changes in aircraft weights do not affect the aircraft balancing so significantly that the planform shall be drastically changed. Generally, minor shifts in the wing position are expected and minor changes in the tail planform sizing could happen, so aircraft empty weights may increase. However, the effects of such changes are assumed to be small in comparison to weight reductions experienced with the HLFC wing.

The transition line for the upper and lower surface of the Fokker F70 is presented in Fig.5(a). In particular, laminar flow is reached for an average of 60% of the chord for the upper surface while approximately 40% for the

DOI: 10.13009/EUCASS2023-377

Table 2: Optimization results for the A220.

	Turbulent opt.	**HLFC opt.**
$C_{L_{cruise}}$	0.4014	0.3769
C_L/C_D	16.3	18.4
$C_{D_{wing}}$	0.0126	0.0106
$\Delta C_{D_{wing}}$		-15.9%
W_w	8502 kg	5787 kg
$W_{b_{power}}$	0 kg	534 kg
$W_{BLS_{tot}}$	0 kg	255 kg
W_{TO}	64379 kg	59757 kg
W_f	12119 kg	10140 kg
ΔW_f		-14.4%

Table 3: Optimization results for the A320.

	Turbulent opt.	**HLFC opt.**
$C_{L_{cruise}}$	0.5092	0.5019
C_L/C_D	18.4	19.3
$C_{D_{wing}}$	0.0160	0.0136
$\Delta C_{D_{wing}}$		-15.0%
W_w	10131 kg	7764 kg
$W_{b_{power}}$	0 kg	411 kg
$W_{BLS_{tot}}$	0 kg	199 kg
W_{TO}	78709 kg	74574 kg
W_f	14709 kg	13215 kg
ΔW_f		-10.2%

bottom one. This configuration, in fact, presents a limited, leading edge sweep angle (20 deg) and 0.73 as the cruise Mach number.

Considering the Airbus A220 in Fig.5(b), laminar flow is limited to 35% for the upper surface, while 25% for the bottom. The Airbus A320 in Fig.5(c) has an analogous laminar portion of the A320 but with improvement for the bottom surface. Both cases present turbulent flow close to the root.

The optimized airfoils for the three aircraft are presented in Fig.6, at different spanwise position (for the F70 the 'kink' position is referred to an intermediate position at about 35% of the span). In particular, the different shapes are due to the different cases applied. In fact, when the turbulent case is adopted, the aerostructural optimization has to find the proper configuration to minimize fuel weight but without any laminar flow, fixing the transition point at the leading edge. In the case of HLFC, the airfoil shape has to be tuned exploiting the significant reduction in drag given by the wing laminarization but without penalizing the potential increment of wing weight.

In a low-fidelity analysis, for example, used as a reference for further analyses, the transition Reynolds Re_T given by the product of the Reynolds number and the transition position chordwise represent useful information to simulate the portion of laminar flow. In this case, the transition is determined when Re_T is reached. Figure 7 shows a series of cases analyzed by Hepperle,[19] readapted in Karpuk et al.[4] and modified in this research with some extra results. The cases studied are for NLF and HLFC applications. Besides, two different bounds are established, the orange curve for NLF and the blue one for HLFC. Especially the last limit represents a quite optimistic prediction. In fact, it is challenging to reach so high Re_T for a practical wing application, considering typical aerostructural and certification limitations. The aircraft analyzed in this research show to be quite far from the HLFC bound. Three different spanwise positions are analyzed for each aircraft, at 15%, 50%, and 75% of the span. The SE^{2}A MR-HLFC case[23] shows that at 15% of the span, the Re_T is getting close to the upper bound. In fact, the position is characterized by a high Reynolds number. Nevertheless, more than 70% of laminar flow (upper surface) is achieved. A complete redesign of the aircraft favors this condition. In fact, the higher freedom of the optimizer in changing the wing geometry allows it to reach better aerodynamic performance.

In Fig.8, linear correlations are shown to determine the transition Reynolds once the leading edge sweep angle is known at different span positions. In particular, in this research, the reader should be aware that to be consistent with data in the literature, upper surface transition data are used to plot the correlations even if the wing presents BLS on both surfaces. Hence, at 15% of the span:

$$Re_T = (-1.0 \cdot \varphi_{LE} + 37.87) \cdot 10^6 \tag{11}$$

DOI: 10.13009/EUCASS2023-377

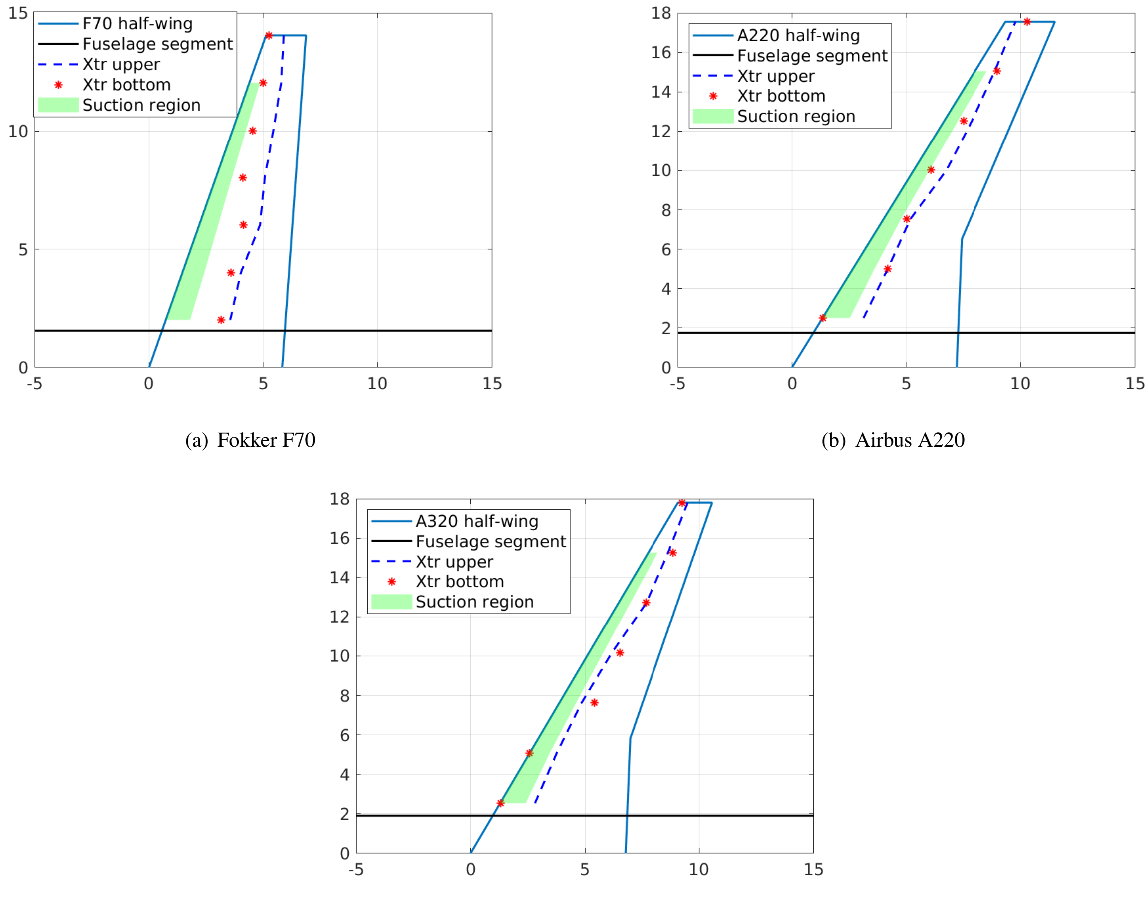

(a) Fokker F70

(b) Airbus A220

(c) Airbus A320

Figure 5: Summary of transition lines for three reference aircraft.

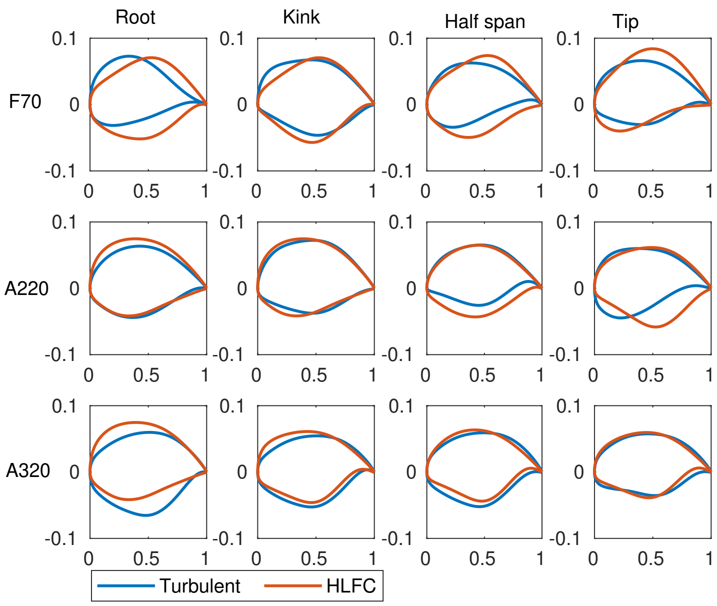

Figure 6: Optimized airfoils for turbulent and HLFC cases, at different spanwise positions.

DOI: 10.13009/EUCASS2023-377

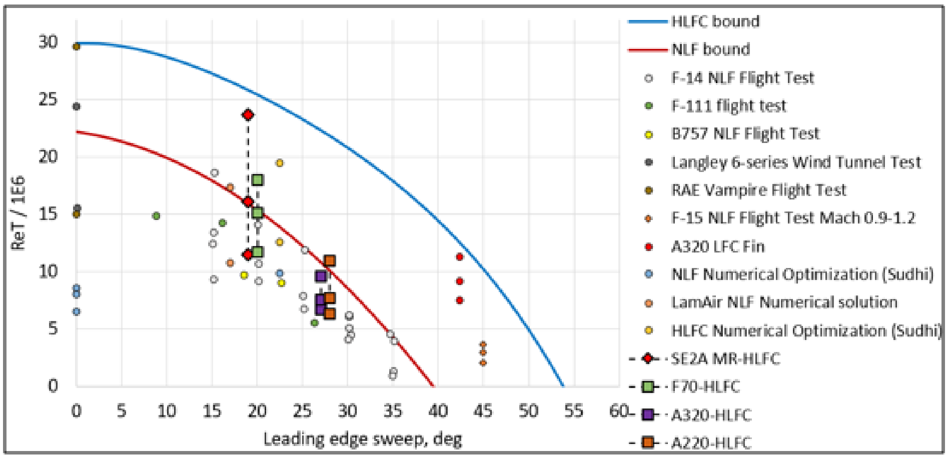

Figure 7: Transition Reynolds number versus leading edge sweep with results of designed HLFC aircraft (adapted from Hepperle[4, 19]).

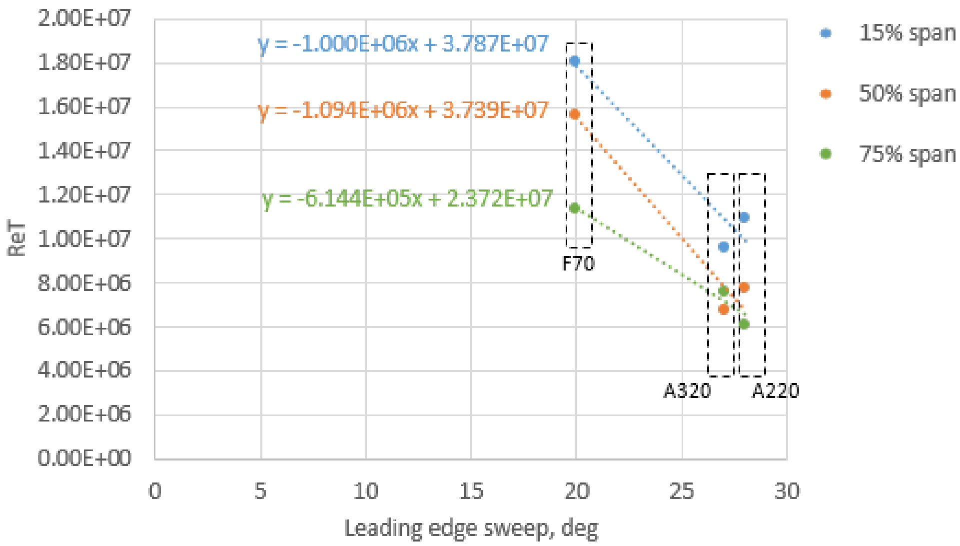

Figure 8: Transition Reynolds number at different span position.

where φ_{LE} represents the leading edge sweep angle. At 50% of the span, the equation becomes:

$$Re_T = (-1.09 \cdot \varphi_{LE} + 37.39) \cdot 10^6 \tag{12}$$

While at 75% of the span:

$$Re_T = (-0.61 \cdot \varphi_{LE} + 23.72) \cdot 10^6 \tag{13}$$

The equations give a first approximation of the value of Reynolds to be used in the early design phase to design aircraft equipped with suction for wing laminarization, following, for example, a procedure like the one shown in Sec.2. Hence, Eq.(4) that represents an upper limit can be replaced by Eqs. (11), (12), (13) for higher accuracy. Once Re_T is found, the transition location can be determined through Eq.(5).

5. Conclusion

The present research investigates the capabilities of hybrid laminar flow control, implementing the technology in existing commercial aircraft and minimizing the variation of the configuration of the aircraft. First, the commercial aircraft are digitized and sized properly according to the mission at a low fidelity level for turbulent and hybrid laminar flow control applications. The use of boundary layer suction technology implies an airfoil variation and hence some variation of the weights. Then a mid-fidelity analysis is performed, optimizing the two different versions of each aircraft.

DOI: 10.13009/EUCASS2023-377

In order to help the optimizer find the solution, preliminary 2d section optimizations are performed according to flight conditions. Once optimized airfoil shapes are found, they are used for full aerostructural optimizations. The optimization framework presents an aerostructural coupling, in which weight estimation is given by physics-based analysis, while the aerodynamics by a quasi-three-dimensional approach. Semi-empirical methodologies are used to evaluate the performance. A genetic algorithm is used. Results show a potential reduction of fuel weight up to 16% optimizing airfoil shape with suction technology with respect to the optimized turbulent configuration. Similar reductions are achieved for wing drag. Limiting the optimizations to an airfoil shape, twist, and suction parameters (if boundary layer suction is applied) as design variables means reducing the potential benefits achievable by suction technology. A correlation between the transition Reynolds and leading edge sweep angle is derived, useful for the preliminary design phase, and data are fitted in to complete existing analysis from literature. Further correlations are developed to distinguish the wing portion interested by laminar flow according to the spanwise position. The research will be followed by future analyses augmenting the number of commercial aircraft tested, including long-range applications.

6. Acknowledgments

We would like to acknowledge the funding by the Deutsche Forschungsgemeinschaft (DFG, German Research Foundation) under Germany's Excellence Strategy—EXC 2163/1-Sustainable and Energy Efficient Aviation—Project-ID 390881007.

References

[1] Flightpath 2050-europe's vision for aviation: Advisory council for aeronautics research in europe, 2011.

[2] P. Horst, A. Elham, and R. Radespiel. Reduction of aircraft drag, loads and mass for energy transition in aeronautics. *Deutsche Gesellschaft für Luft- und Raumfahrt - Lilienthal-Oberth e.V.*, 2021.

[3] N. Beck, T. Landa, A. Seitz, L. Boermans, Y. Liu, and R. Radespiel. Drag reduction by laminar flow control. *Energies*, 11(252), 2018.

[4] S. Karpuk, R. Radespiel, and A. Elham. Assessment of future airframe and propulsion technologies on sustainability of next-generation mid-range aircraft. *Aerospace*, 9(5), 2022.

[5] Bertram O. Krishnan, K.S.G. and O. Seibel. Review of hybrid laminar flow control systems. *Progress in Aerospace Sciences*, 93:24–52, 2017.

[6] R. Henke. "a 320 hlf fin " flight tests completed. *Air Space Europe*, 1(2):76–79, 1999.

[7] A. Sudhi, A. Elham, and C. Badrya. Coupled boundary layer suction and airfoil shape optimization for hlfc application. *AIAA J.*, 2021.

[8] A. Sudhi, R. Radespiel, and C. Badrya. Design exploration of transonic airfoils for natural and hybrid laminar flow control applications. *Journal of Aircraft*, 0(0):1–17, 0.

[9] V. Mosca, S. Karpuk, A. Sudhi, C. Badrya, and A. Elham. Multidisciplinary design optimisation of a fully electric regional aircraft wing with active flow control technology. *The Aeronautical Journal*, pages 1–25, 2021.

[10] G. K. W. Kenway, G. J. Kennedy, and J. R. R. A. Martins. Scalable parallel approach for high-fidelity steady-state aeroelastic analysis and adjoint derivative computations. *AIAA J*, 52(5), 2014.

[11] E. Obert. *Aerodynamic Design of Transport Aircraft*. IOS Press BV, Netherlands, 2009.

[12] T. Lukaczyk, A. Wendroff, M. Colonno, T. Economon, J. Alonso, and T. Orra. Suave: An open-source environment for multi-fidelity conceptual vehicle design. *16th AIAA ISSMO Multidisciplinary Analysis and Optimization Conference*, 22-26 June 2015.

[13] S. Gudmundsson. *General Aviation Aircraft Design: Applied Methods and Procedures*. Butterworth-Heinemann, Oxford, UK, 1 edition, 2013.

[14] M. Drela and H. Youungren. Athena vortex-lattice method. *Massachusetts Inst. of Technology, Cambridge, MA*, 2020.

DOI: 10.13009/EUCASS2023-377

[15] R. Shevell and F. Bayan. Development of a method for predicting the drag divergence mach number and the drag due to compressibility for conventional and supercritical wings. *Research Report SUDAAR 522*, 1980.

[16] D. Scholz. *Aircraft Design -an Open Educational Resource (OER) for Hamburg Open Online University (HOOU)*. 2021.

[17] A. Elham, G. La Rocca, and M. J.L. Van Tooren. Development and implementation of an advanced, design-sensitive method for wing weight estimation. *Aerospace Science and Technology*, 29(1):100–113, 2013.

[18] D. Wells, B. Horvath, and L. McCullers. The flight optimization system weights estimation method. *TM 20170005851*, 11(1), 2017.

[19] M. Hepperle. Mdo of forward swept wings. *In Proceedings of the AKATnet II Workshop*, 2008.

[20] S. Powell and A. Sóbestery. Application-specific class functions for the kulfan transformation of airfoils. *13th AIAA/ISSMO Multidisciplinary Analysis and Optimization Conference 2010*, 2010.

[21] B. Kulfan. A universal parametric geometry representation method - "cst". *45th AIAA Aerospace Sciences Meeting and Exhibit, American Institute of Aeronautics and Astronautics*, 2007.

[22] A.B. Lambe and J.R.R.A. Martins. Extensions to the design structure matrix for the description of multidisciplinary design, analysis, and optimization processes. *Struct. Multidiscip. Des. Optim.*, 46,:273–284, 2012.

[23] V. Mosca, A. Sudhi, C. Badrya, and A. Elham. Multidisciplinary design optimization of transonic wings with boundary layer suction. 2022.

[24] Certification specifications and acceptable means of compliance for large aeroplanes cs-25. 2020.

[25] J. Mariens, A. Elham, and M. J.L. Van Tooren. Quasi-three-dimensional aerodynamic solver for multidisciplinary design optimization of lifting surfaces. *Journal of Aircraft*, 51(2):547–558, 2014.

[26] T. Streit, S. Wedler, and M. Kruse. Dlr natural and hybrid transonic laminar wing design incorporating new methodologies. *The Aeronautical Journal*, 119(1221):1303–1326, 2015.

[27] K. Risse. Preliminary overall aircraft design with hybrid laminar flow control. *Phd thesis*, 2016.

[28] M. Drela. Design and optimization method for multi-element airfoils. *Aerospace Design Conference*, 1993.

[29] G. Schrauf. Coco-a program to compute velocity and temperature profiles for local and non local stability analysis of compressible, conical boundary layers with suction. *ZARM Technik report*, 1998.

[30] G. Schrauf. Lilo 2.1 user's guide and tutorial. *GSSC Technical Report*, 6, 2006.

[31] W. Pfenninger. Some results from the x-21a program. part i: Flow phenomena at the leading edge of swept wings. *AGARDograph*, 97(4):1–41, 1965.

[32] W. Pfenninger. Laminar flow control—laminarization. *Special Course on Concepts for Drag Reduction*, AGARD-R-654, NATO AGARD:3.1–3.75, 1977.

[33] S. Karpuk and A. Elham. Influence of novel airframe technologies on the feasibility of fully-electric regional aviation. *Aerospace*, 8(6), 2021.

[34] V. Iyer and O. Bertram. Assessment of a chamberless active hlfc system for the vertical tail plane of a mid-range transport aircraft. *Deutscher Luft- und Raumfahrtkongress*, 2017.

[35] G. Kalarikovilagam Srinivasan and O. Bertram. Preliminary design and system considerations for an active hybrid laminar flow control system. *Aerospace*, 6(10):109, Oct 2019.

[36] J. Roskam. *Airplane design, Part, I: Preliminary sizing of airplanes*. DARcorporation, Lawrence Kansas, 1986.